

RSC Advances



This is an *Accepted Manuscript*, which has been through the Royal Society of Chemistry peer review process and has been accepted for publication.

Accepted Manuscripts are published online shortly after acceptance, before technical editing, formatting and proof reading. Using this free service, authors can make their results available to the community, in citable form, before we publish the edited article. This *Accepted Manuscript* will be replaced by the edited, formatted and paginated article as soon as this is available.

You can find more information about *Accepted Manuscripts* in the [Information for Authors](#).

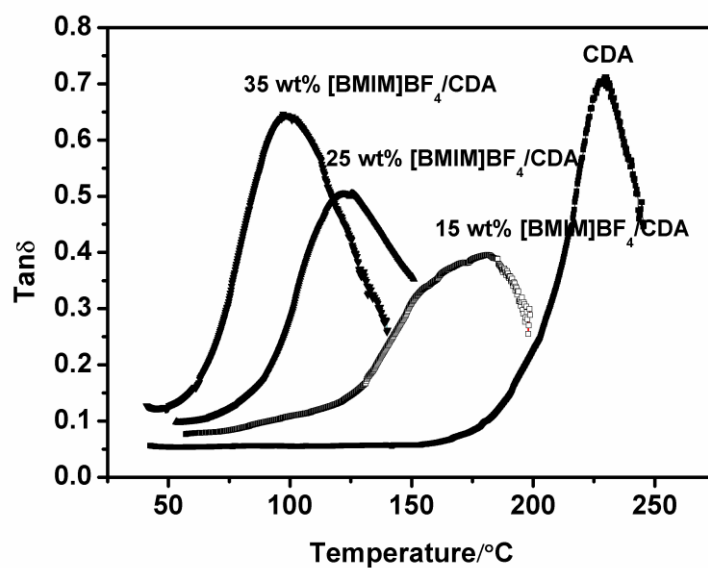
Please note that technical editing may introduce minor changes to the text and/or graphics, which may alter content. The journal's standard [Terms & Conditions](#) and the [Ethical guidelines](#) still apply. In no event shall the Royal Society of Chemistry be held responsible for any errors or omissions in this *Accepted Manuscript* or any consequences arising from the use of any information it contains.

Thermal Behaviors of Cellulose Diacetate Melt Using Ionic Liquids as a Plasticizer

Zhixing Li, Na Liu, Yongbo Yao, Shiyang Chen*, Haifeng Wang and Huaping Wang*

State Key Laboratory for Modification of Chemical Fibers and Polymer Materials, Key Laboratory of High Performance Fibers and Products (Ministry of Education), College of Materials Science and Engineering, Donghua University, Shanghai 201620, China

E-mail: chensy@dhu.edu.cn; wanghp@dhu.edu.cn; Tel: +862167792950, Fax: +862167792958



Thermal Behaviors of Cellulose Diacetate Melt Using Ionic Liquids as a Plasticizer

Zhixing Li, Na Liu, Yongbo Yao, Shiyan Chen*, Haifeng Wang and Huaping Wang*

State Key Laboratory for Modification of Chemical Fibers and Polymer Materials, Key Laboratory of High Performance Fibers and Products (Ministry of Education), College of Materials Science and Engineering, Donghua University, Shanghai 201620, China

E-mail: chensy@dhu.edu.cn; wanghp@dhu.edu.cn; Tel: +862167792950, Fax: +862167792958

The 1-butyl-3-methylimidazolium tetrafluoroborate ([BMIM]BF₄) was chosen as the plasticizer of cellulose diacetate (CDA) to investigate the feasibility of CDA melt spinning. The [BMIM]BF₄/CDA was characterized by the fourier transform infrared (FTIR), the dynamic thermomechanical analysis (TG), the degree of crystallinity (XRD), the Scanning electron micrographs (SEM) and the thermal stability of CDA. The rheological properties of [BMIM]BF₄/CDA were investigated by rotary rheometer and the zero-shear viscosity was predicted by the three-parameter Carreau viscosity model from the apparent viscosity data. The [BMIM]BF₄/CDA melt showed shear-thinning behaviours. The melt with higher CDA concentration and higher shear rate were found to be sensitive to the temperature, so we can adjust processing technology by changing temperature and shear rate. However, the structural viscosity index of the melt decreased with the increase of the [BMIM]BF₄ content and went up after a decline with the temperature increase.

Introduction

As one of cellulose derivatives, CDA have been widely applied as the materials of CDA fibers for cigarette filter and textile. Owing to the intermolecular and intramolecular hydrogen bonds in CDA, they are got the high viscosity and elevated glass transition temperature, and not processable as a thermoplastic [1-3]. As we all know, the conventional method for manufacturing CDA fibers was solution spinning including wet spinning and dry spinning [4], where a large

amount of deleterious solvents were used such as acetone. The melt spinning process is a method with high production efficiency, so the melt spinning process of CDA fibers have attracted wide spread attention at home and abroad.

In an effort to modify its properties and facilitate processing, CDA was modified through varying plasticizer such as various aliphatic and aromatic esters [5-8], physical plasticizing etc. Lee et al. [9] researched that the glass transition temperature (T_g) of CDA can be reduced to 80–100°C by adding maleic anhydride, glycerol and citrate esters. Meanwhile, Zepnik et al. [10] have recently studied the effect of plasticizer type and concentration on CDA using benzoate, acetates, phosphate and citrates based plasticizers. An increase in plasticizer concentration resulted in significant broadening of the thermoplastic processing window due to a strong decrease in glass transition temperature. Similar trend of CDA stiffness and toughness properties was observed [11]. Besides, the chemical plasticizing was used to being applied. Szamel et al. [12] used caprolactone as an internal plasticizer, which changed the molecular structure of CDA. According to the activity of the molecular chain of CDA, they found that it was better to use caprolactone as internal plasticizer than to be as external plasticizer. CDA also could be successfully plasticized by grafting PLA, which realized melt process without any external plasticizer [13-14]. Luan et al. [15] used method called “one pot” to prepare thermoplastic CDA-graft-poly(L-lactide) copolymers from unmodified cellulose in ILs ([Amim]Cl). The thermoplastic copolymers could be processed by conventional hot working so as injection and melt spinning. However, the former conventional plasticizers usually have problems like toxicity [16], changing the structure of cellulose acetate or arising leakage during machining process because of the compatibility.

ILs containing imidazolium or pyridinium cations like some conventional plasticizers, containing an aromatic core and pendant alkyl groups. Due to its excellent advantages such as environmentally friendly, no detectable vapor pressure, high thermal stability and low temperature stability, polar and acidic adjustable, small evaporation losses, Ionic liquids (ILs) [17-18] have attracted an interest in the material, chemical industry and various fields. Because they have good compatibility with polymer, endowed the polymer better stability, enlarged the adjusting range of modulus of elasticity, made the plasticizing polymer glass transition temperature lower [19-20], ILs may have potential application as plasticizer. [BMIM]BF₄ is one of the most used ILs which has a wide temperature range [21].

In this paper, we chose [BMIM]BF₄ as the plasticizer to achieve the CDA melt spinning, and studied the steady and dynamic-state rheological properties of CDA/ILs melt in order to guide for processing and predict its spinnability.

Experimental

Materials and methods

The CDA were provided by Nantong Acetate Fiber Company Limited. Its degree of polymerization is 300, and the DS is 2.4. [BMIM]BF₄ was provided by ionic liquid-Shanghai Cheng Jie Chemical Company Limited. FTIR of the blends were recorded with a Nicolet FTIR spectrometer (Nexus 670, Thermo Fisher, USA) at wavenumber of 700–4,000 cm⁻¹. Scanning electron micrographs (SEM) were taken on SU8010 Field Emission Scanning Electron Microscope. The cellulose diacetate films were frozen in liquid nitrogen and fractured. The fractured surface of the film was sputtered with gold and then observed. X-ray diffraction patterns were recorded in the reflection mode in the angular range of 3–60° (2 θ) at ambient temperature by an X'Pert Pro MPD diffractometer. The radiation from the anode, operating at 50 KV and 35 mA monochromized with a nickel foil. DMA of [BMIM]BF₄/CDA films were tested at a heating rate 5 °C /min from 40 to 300 °C under 1Hz in dynamic mode according to TA Q800 from America. The thermal decomposition studies of CDA films were carried out on American TA Q5000IR instrument under a nitrogen environment (50 mL/min) at a heating rate 10 °C /min from 40 to 600 °C. Each film was tested at least three times to confirm the reproducibility of the data. The steady-state and dynamic rheological measurements were performed on ARES-G1 (TA, American) equipped with 25.0 mm parallel plates fixture. The steady state sweeps were conducted for different [BMIM]BF₄/CDA over the range of shear rate of 0.01-100 s⁻¹ at 170 °C, 180 °C, 190 °C and 200 °C.

[BMIM]BF₄/CDA film preparation

CDA powder was dried in the vacuum oven for 24 hours at 60°C, 15wt%, 25wt% and 35wt% [BMIM]BF₄/CDA were dissolved in acetone to acquire 20 wt% acetone solution. The mixture was stirred for 2 h to prepare a homogenous paste. After completely dissolved, the films of 0.1mm thickness were prepared using a film making instrument. The films were dried in a vacuum oven at 60 °C for 12 h to remove acetone.

[BMIM]BF₄/CDA tablet preparation

CDA powder was dried in the vacuum oven for 24 h at 60°C, 15wt%, 25wt% and 35wt% [BMIM]BF₄/CDA were mixed in a high-speed mixer and then make 25.0 mm diameter and 1.0 mm thickness using tablet compressing machine at room temperature to make sure there is no thermal history before test [22].

Results and discussion

FTIR characterization of [BMIM]BF₄/CDA

To understand the structure of the [BMIM]BF₄/CDA, Figure 1 shows the FTIR spectra of the original CDA, virgin [BMIM]BF₄ and 25 wt% [BMIM]BF₄/CDA. The absorption peak of '-OH' is at 3480 cm⁻¹, and the absorption peak of [CH₃COO] (C=O, C-O, C-H) are at 1743, 1369 and 1230 cm⁻¹, respectively. The absorption peak of [BF₄]⁻ anions and imidazolium rings are observed at approximately 2970, 1571, 1462, 1200, and 1000 cm⁻¹, respectively. The blends of [BMIM]BF₄/CDA shows the decrease of hydroxyl from the weaker peak at 3528 cm⁻¹ [23]. FTIR can also be used to study the hydrogen bonds in the infrared region by the vibrations of molecules. Figure 2 shows the magnified FTIR spectra between 4000-3000 cm⁻¹. There is no absorption band of free hydroxyl groups at 3600 cm⁻¹ for CDA which means that the hydroxyl groups are associated with the intermolecular or intramolecular hydrogen bonds in CDA [24]. The absorption peak of hydroxyl group would move to lower frequency (3480 cm⁻¹) when the hydrogen bonds form by the hydroxyl groups. With the increase of [BMIM]BF₄ content, the absorption peak of hydrogen bonds shifts to higher value and the intensity decreases. The frequency shifts indicate that the hydrogen bonds become weak. Moreover, the intensity of the peak is proportional to the strength of the hydrogen bonds. It can be explained that stronger interactions between [BMIM]⁺, [BF₄]⁻ in [BMIM]BF₄ and CDA molecule form, thus break the hydrogen bonds between the hydroxyl group of CDA molecules. This provides a new way to plasticize CDA like glycerol which can form stronger interaction to weaken the hydrogen bonds [25].

The effect of [BMIM]BF₄ on the crystalline property of CDA

To investigate the effect of [BMIM]BF₄ on the crystalline property of CDA, the XRD measurements were performed. The obtained XRD patterns of pure CDA and CDA plasticized with different content of [BMIM]BF₄ are shown in Figure 3. On the XRD curve of pure CDA, the diffraction peaks at 2θ = 17.12 of 021, 2θ = 10.42 of 210 for CDA are observed [26]. No new crystalline peaks appeared on the XRD curves of the [BMIM]BF₄ plasticized CDA. This indicated that the type of CDA crystals were not affected by the addition of [BMIM]BF₄. The diffraction peaks of CDA decreased rapidly in intensity with the addition of [BMIM]BF₄ and almost disappeared when added with 35 wt% [BMIM]BF₄. This demonstrated that [BMIM]BF₄ would effectively decrease the degree of crystallinity of CDA.

The morphology of the mixture of [BMIM]BF₄/CDA

To understand the phase morphology well of [BMIM]BF₄/CDA, the morphology of blends fractured surface were characterized by SEM shown in Figure 4. The surface of CDA presents a classical reticular structure of the microporous

membrane (Figure 4a). After adding the ILs, the structure of the system transformed from the microporous structure of CDA to rough structure (15 wt% [BMIM]BF₄/CDA and 25 wt% [BMIM]BF₄/CDA), then to almost a smoothly homogeneous phase structure (35 wt% [BMIM]BF₄/CDA). As a good kind of solvent for CDA [21], the more [BMIM]BF₄ would make the system to form a better homogenous phase which would affected crystallinity of CDA. It is confirmed by the results from the XRD data. The results indicated that [BMIM]BF₄ played an important role on the structure of films to change phase.

Thermal properties of [BMIM]BF₄/CDA

T_g is important for design of polymeric materials because it is related to the transition between hard, glassy properties at lower temperatures and rubbery behavior at higher temperatures. The stiffness of CDA is mainly due to the existence of the strong intermolecular hydrogen bonds. We chose [BMIM]BF₄ as a kind of physical plasticizer to decrease the temperature of processing. Glass transition temperatures were determined by DMA. Figure 5 shows the relationship between Tanδ and temperature. Tanδ is a damping term defined as the ration of energy dissipated as heat to the maximum energy stored in the material. It is an index of material viscoelasticity. The temperature of the peak is related to the glass transition temperature (T_g). As shown in Figure 5, the T_g of CDA significantly decreased from 225 °C to 95 °C when the [BMIM]BF₄ content increases from 0 wt% to 35 wt% in [BMIM]BF₄/CDA. The [BMIM]BF₄ plasticizes CDA by breaking the hydrogen bonds between CDA molecules with [BF₄]⁻. The more hydrogen bonds are broken, the more molecular chain move easily, which presents the decrease of T_g [27-31]. The optimum plasticizer concentration is key parameter to reduce the processing temperature without compromising the stability and other performances of CDA. The phenomenon demonstrated that [BMIM]BF₄ plasticizer can successfully decline T_g of CDA and make CDA workable and flexible at lower temperatures.

The obtained TGA curves of pure CDA and [BMIM]BF₄ plasticized CDA are shown in Figure 6(a). The shape of mass loss curves for pure CDA is consistent with the generally accepted one-step mechanism for the thermal degradation of CDA [32-33]. While the mass loss curves for adding [BMIM]BF₄ are consistent with the two steps according to the Figure 6(b). It is clearly shown that the addition of [BMIM]BF₄ would decrease the thermal stability of CDA. The T_d value decreased from 375 °C of pure CDA to 330°C with 35 wt% [BMIM]BF₄. The thermal degradation of CDA extends to the amorphous phase after adding [BMIM]BF₄. With the addition of [BMIM]BF₄, the crystals of CDA would be

destroyed and the degree of crystallinity of CDA decreased (XRD characterization). The amorphous CDA would be easier to start the thermal degradation and thus showed a lower thermal stability.

Steady shear rheological behaviors of [BMIM]BF₄/CDA melt.

The effect of plasticizer on melt viscosity of the [BMIM]BF₄/CDA blends were evaluated in apparent viscosity at different temperature and different content. Figure 7 presents the curves of apparent viscosity versus shear rates for 25 wt% [BMIM]BF₄/CDA samples at temperature of 170-200°C. The blends exhibit typical shear-thinning characteristic, i.e. decrease of viscosity with increase of shear rate, which result from the unlocking the tangles of molecular chain and orienting in the direction of the shear. The influence of [BIMI]BF₄ is more obvious in the lower shear rate range, whereas at higher shear rate, the influence diminishes due to the shear thinning effect of the polymer melt [34]. Besides, the apparent viscosity of 25 wt% [BMIM]BF₄/CDA decrease with the increase of temperature because more energy is provided for the molecules with the increase of temperature [35]. Moreover, the Carreau model fitting parameters (Table 1) represents the zero shear rate viscosity and the power-law exponent decreased with the increase of temperature. The decreasing power-law exponent indicates high deviation from Newtonian fluids of [BMIM]BF₄/CDA melt.

As shown in Figure 8, the [BMIM]BF₄/CDA blends were evaluated in apparent viscosity by a function of different shear rate at 190°C. Increasing content of the [BMIM]BF₄ resulted in consistent decrease in apparent viscosity. This retrogression in apparent viscosity indicated that macromolecular chain changed to move more easily during the compounding process. This phenomenon is according to the previous results of the decrease in T_g from the DMA test. Table 2 presents the zero shear rate viscosity decrease while the power-law exponent increase with the increase of content of [BMIM]BF₄.

The three-parameter Carreau viscosity model was used to express the changes from the Newton region to non-Newton region and predict the zero-shear viscosity from the apparent viscosity data. The three-parameter Carreau viscosity model was given by Eq. 1[36]:

$$\eta = \frac{\eta_0}{[1+(\lambda\dot{\gamma})^2]^{\frac{1-n}{2}}} \quad (1)$$

$\dot{\gamma}$ is the shear rate, η_0 is the zero shear rate viscosity, λ is a constant with the relaxation time in seconds and N is the power-law exponent.

The temperature of the experiment is above the glass transition temperature of polymer melt, where the relationship of viscosity and temperature usually follows the Arrhenius equation to a good approximation. The Arrhenius equation was given by Eq. 2[37]:

$$\eta_a = Ae^{E_\eta/RT} \quad (2)$$

In this equation, η_a is the viscosity at temperature T , E_η is flow activation energy, which represents the sensitivity of viscosity to temperature, A is a constant characteristic of polymer and its molecular weight, R is the universal gas law constant, and T is the absolute temperature, R_0 is correlation coefficient. The Arrhenius plot of $\ln\eta_a$ versus $1/T$ was shown in Figure 9. From the slope of the linear fit, the flow activation energy E_η can be calculated and the data are shown in the Table 3.

As we know, E_η is that one molecule needs the energy to overcome interaction between molecules to change its position. It is a significant factor in processing especially spinning. Figure 8 calculates the viscous flow activation energy by using Arrhenius Equation at different shear rate and the data are listed in Table 3. From the data, we can see that the E_η decreases from 128 kJ/mol to 66 kJ/mol when the shear rate increases from 0 s^{-1} to 10 s^{-1} . Figure 10 and Table 4 show that E_η decrease with the increase of the [BMIM]BF₄ content, which means that viscosity is sensitive to the temperature. So the viscosity of the [BMIM]BF₄/CDA melt could be regulated by temperature, shear rate and the [BMIM]BF₄ content.

Effect of temperature and concentration on structural viscosity index

Structural viscosity index characterizing the structure degree of the polymer fluid is an important parameter measuring the spinnability of the spinning fluid. In addition, it reflects the entanglement degree of internal macromolecular chains of the fluid. Structural viscosity index is defined by the following Eq. 3[38]:

$$\Delta\eta = -\left(\frac{d\log\eta_a}{d\dot{\gamma}^{1/2}}\right) \quad (3)$$

In this equation, $\Delta\eta$ is the structural viscosity index, η_a is the apparent viscosity, $\dot{\gamma}$ is the shear rate. The structural viscosity index $\Delta\eta$ in the area of non-Newtonian is $\Delta\eta > 0$. The smaller the structural viscosity index $\Delta\eta$ is, the lower structuredness of the spinning fluid is. This indicated the spinnability of the fluid was excellent. The structural viscosity indexes showed at different temperatures for 25 wt% [BMIM]BF₄/CDA melt in Figure 11 (a) and with different concentrations at 190 °C in Figure 11 (b).

As shown in the inset of Figure 11 (a), the structural viscosity index first decreases and then increases with the increase of the temperature. It is known that the melt can be seen as a kind of network structure. The apparent viscosity decreases with the increase of the shear rate. When the shear rates were fixed, the shear-thinning tendency was only concerned with the macromolecular interaction. When the temperature increased, this kind of interaction become smaller, which made the structural viscosity index become smaller. Some crosslinking and degradation would occur, when the temperature got as high as to 200 °C. The apparent viscosity becomes sensitive to the shear rate and the structural viscosity index increases. Therefore, the appropriate temperature for melt spinning of [BMIM]BF₄/CDA melt was 190 °C from the rheological experiments, which will be further confirmed in the spinning process. Figure 11 (b) shows the structural viscosity indexes decrease with the increase of the content of [BMIM]BF₄. The macromolecular interaction become smaller because of the smaller content of CDA, which result in the decrease of the structural viscosity index.

Conclusions

In conclusion, we discussed the feasibility of CDA using [BMIM]BF₄ as the plasticizer. [BMIM]BF₄ could strongly interact with CDA molecule and reduce the intensity of the hydrogen bonds between CDA molecules. Moreover, [BMIM]BF₄ could effectively destroy the crystallization of CDA and decreased its crystallinity, thus the thermal stability decreased with adding [BMIM]BF₄. The surfaces of [BMIM]BF₄/CDA films became smooth and formed the homogeneous phase with the increasing of [BMIM]BF₄. Further, the steady rheological behaviors of [BMIM]BF₄/CDA were studied at different temperature and concentration. The results demonstrated that zero-shear viscosity decreased and power-law index increased with the increase of the [BMIM]BF₄ content at the same temperature. The flow activation energy decreased with the increase of shear rate. In total, the system of [BMIM]BF₄/CDA was sensitive to the temperature. However, the structural viscosity index decreased and then increased with the increase of the temperature, which indicated 190 °C was the optimum melt-spun temperature. The investigation provided guidance for CDA melt spinning using [BMIM]BF₄ as the plasticizer.

Acknowledgements

This work is supported by a grant from National Natural Science Foundation of China (51273041) and the Fundamental Research Funds for the Central Universities (2232013D3-01).

References

- 1 Johannes, S. and Florian, F. *Cellulose*, 2006, 159-165.
- 2 Richard, D. and Richard, A. *Journal of Apply Polymer Science*, 1999, **77**, 418-423.
- 3 Zugenmaier, P. *Macromolecular Symposia*, 2004, **208**, 81–166.
- 4 Rachel, C. *Macromolecular Symposia*, 2004, **208**, 255-265.
- 5 Yoshioka, M.; Hagiwara, N. and Shiraishi, N. *Cellulose*, 1999, **6**, 193–212.
- 6 Quintana, R.; Persenaire, O.; Bonnaud, L and Dubois, P. *Polymer Chemistry*, 2012, **3**, 591–595.
- 7 Amim, L.; Blachechen, D. and Petri, J. *Thermal Analysis and Calorimetry*, 2012, **107**, 1259–1265.
- 8 Roy, D.; Semsarilar, M.; Guthrie, J.T. and Perrier, S. *Chemical Society Research*, 2009, **38**, 2046–2064.
- 9 Lee, C.; Cho. M.; Kim, I.; Nam, J. and Lee, Y. *Polymer Korea*, 2009, **33**, 243-247.
- 10 Zepnik, S.; Kabasci, S; Radusch, H. and Thomas, W. *Materials Science and Engineering A* , 2012, **2**, 152–163.
- 11 Mohanty, A. K.; Wibowo, A.; Misra, M. and Drzal, L.T. *Polymer Engineering and Science*, 2003, **43**, 1151–1161.
- 12 Szamel, G.; Domjan, A. and Klebert, S. *European Polymer Journal*, 2008, **44**, 357-365.
- 13 Teramoto, Y. and Nishio, N. *Polymer*, 2003, **44**, 2701-2709.
- 14 Teramoto, Y. and Nishio, N. *Biomacromolecules*, 2004, **5**, 397-406.
- 15 Luan, Y.; Wu, J.; Zhan, M.; Zhang, J.; Zhang, J. and He, J. *Cellulose*, 2013, **20**, 327-337.
- 16 Gan, L. M.; Liu, J.; Poon, L. P. Chew, C.H. and Gan, L. H. *Polymer*, 1997, **38**, 5339-5345.
- 17 Esteban, C. and Javier, R. *Journal of Molecular Liquids*, 2011, **163**, 64-69.
- 18 Hui, W.; Gabriela, G. and Robin, D. R. *Chemical Society Reviews*, 2012, **41**, 1519-1537.
- 19 Scott, M.; Rahman, M. and Brazel, C. *European Polymer Journal*, 2003, **39**, 1947-1953.
- 20 Scott, M.; Benton, M.; Rahman, M. and Brazel, C. S. *Ionic liquids as green solvents: progress and prospects*, 2003, **856**, 468-477.
- 21 Sun, D. and Zhou, J. *AIChE Journal*, 2013, **59**, 2630-2639.
- 22 Tian, Y.; Han, K.; Qin, H.; Rong, H.; Yan, B.; Wang, D.; Liu, S. and Yu, M. *Advanced Materials Research*, 2012, **476**, 2151-2157.
- 23 Kareem, T. A. and Kaliani, A. A. *Ionics*, 2013, **19**, 1559–1565.
- 24 Dai, L. and Ying, L. *Macromolecular Materials and Engineering*, 2002, **287**, 509-514.
- 25 Jiang, X.; Jiang, T. and Zhang, X. *Polymer Engineering and Science*, 2013, 1181-1186.

- 26 Qi, S.; Sun, N.; Zhao, B. and Hu, P. *Guangzhou Chemistry*, 1993, 47-52.
- 27 Zhang, H.; Wu, J.; Zhang, J. and He, J. *Macromolecules*, 2005, **38**, 8272-8277.
- 28 Kuo, S.W. and Tsai, H. T. *Macromolecules*, 2009, **42**, 4701–4711.
- 29 Gioia, L. D., Cuq, B. and Guilbert, S. *International Journal of Biological Macromolecules*, 1999, **24**, 341–350.
- 30 Shtarkman B. P. and Razinskaya, I. N. *Acta Polymerica*, 1983, **34**, 514–520.
- 31 Sothornvit, R. and Krochta, J. *Journal of Food Engineering*, 2001, **50**, 149–155.
- 32 Maria, C. and Ana, V. *Polymer Degradation and Stability*, 2003, 149-155.
- 33 Sabyasachi, G.; Laurie, M. and Patrick, R. *Journal of Analytical and Applied Pyrolysis*, 2012. **90**, 33-41.
- 34 Ding, Y.; Peng, N. and Chung, T. *Journal of Membrane Science*, 2011, **380**, 87-97.
- 35 Brrnes, H. A.; Hutt, J. F. and Walter, K. An Introduction to Rheology. *Elsevier Science Publishers: Amsterdam*, 1989, 170-201.
- 36 Zhu, X.; Chen, X. and Wang, X. *Polymer Advance Technology*, 2013, **24**, 90-96.
- 37 Laidler, K. *Journal of Chemical Education*, 1984, **61**, 494-98.
- 38 Cai, J.; Fei, P.; Xiong, Z.; Shi, Y.; Yan, K.; Xiong, H. *Carbohydrate Polymers*, 2013, **92**, 11-18.

Figure and Table

Figure 1 FTIR spectra of CDA, [BMIM]BF₄ and 25 wt% [BMIM]BF₄ in [BMIM]BF₄/CDA.

Figure 2 FTIR spectra of CDA, 15 wt%, 25 wt%, 35 wt% [BMIM]BF₄ in [BMIM]BF₄/CDA.

Figure 3 XRD curves of pure CDA and [BMIM]BF₄/CDA with different [BMIM]BF₄ content.

Figure 4 SEM of pure CDA and [BMIM]BF₄/CDA with different [BMIM]BF₄ content. (a) CDA, (b) 15 wt% [BMIM]BF₄/CDA, (c) 25 wt% [BMIM]BF₄/CDA, (d) 35 wt% [BMIM]BF₄/CDA.

Figure 5 DMA data for different [BMIM]BF₄ content in [BMIM]BF₄/CDA.

Figure 6 TG data (a) and DTG data (b) of films containing different content of [BMIM]BF₄. (1) CDA, (2) 15 wt% [BMIM]BF₄ in [BMIM]BF₄/CDA, (3) 25 wt% [BMIM]BF₄ in [BMIM]BF₄/CDA, (4) 35 wt% [BMIM]BF₄ in [BMIM]BF₄/CDA.

Figure 7 Apparent viscosity curves and Carreau model fitting curves for 25 wt% [BMIM]BF₄ in [BMIM]BF₄/CDA .

Figure 8 Apparent viscosity curves and Carreau model fitting curves at 190 °C.

Figure 9 Calculated the viscous flow activation energy by using Arrhenius Equation at different shear rate.

Figure 10 Calculated the viscous flow activation energy by using Arrhenius Equation for different [BMIM]BF₄ content at 1s⁻¹.

Figure 11. (a) Fitting figure of $\text{Log}\eta_a$ and $\dot{\gamma}^{1/2}$ for 25 wt% [BMIM]BF₄/CDA at different temperatures. Insets shows the structural viscosity indexes; (b) Fitting figure of $\text{Log}\eta_a$ and $\dot{\gamma}^{1/2}$ for [BMIM]BF₄/CDA with different concentrations at 190 °C. Inset shows the structural viscosity indexes.

Table 1. Carreau model fitting parameters for 25 wt% [BMIM]BF₄ in [BMIM]BF₄/CDA.

Table 2. Carreau model fitting parameters at 190°C.

Table 3 The viscous flow activation energy at different shear rate.

Table 4 The viscosity flow activation energy for different [BMIM]BF₄ content at 1s⁻¹.

Figure 1

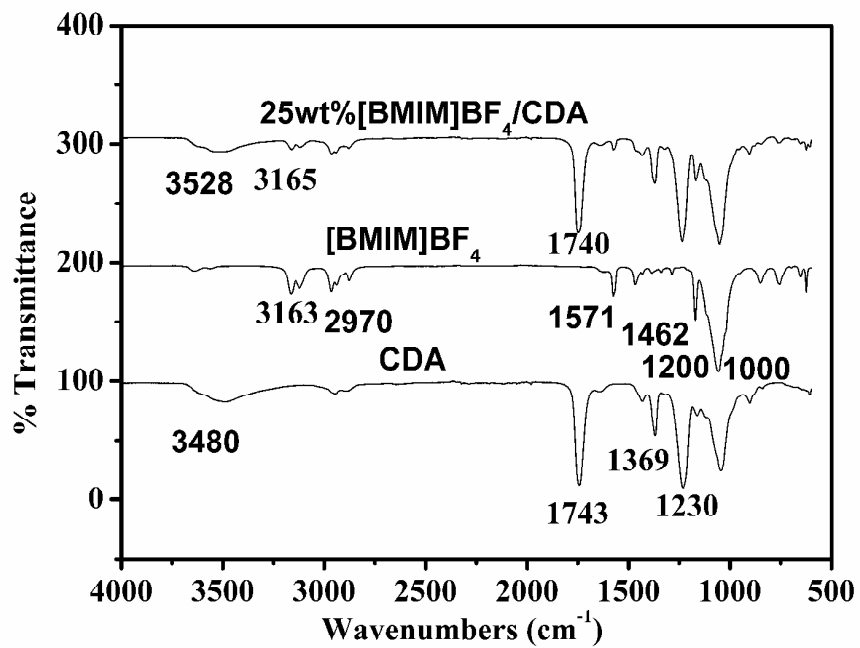


Figure 2

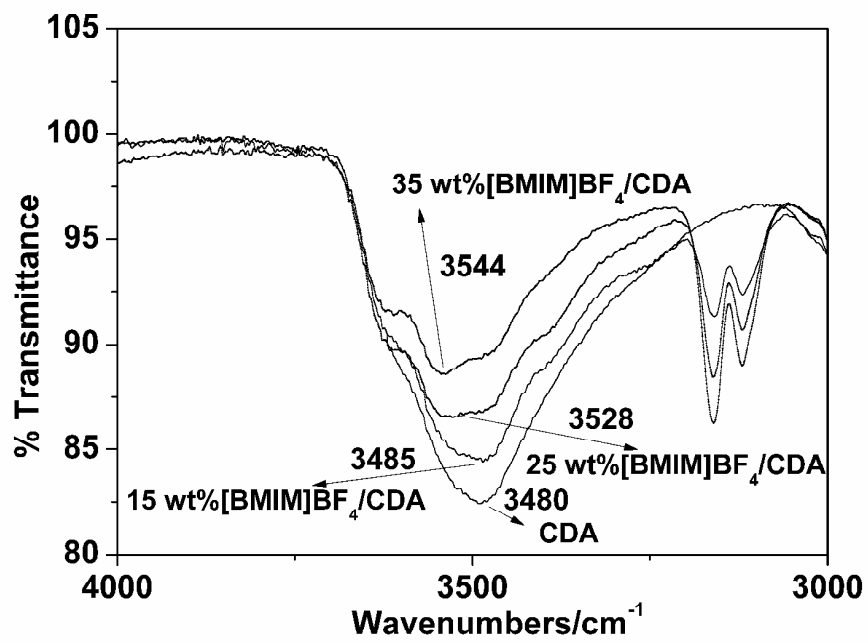


Figure 3

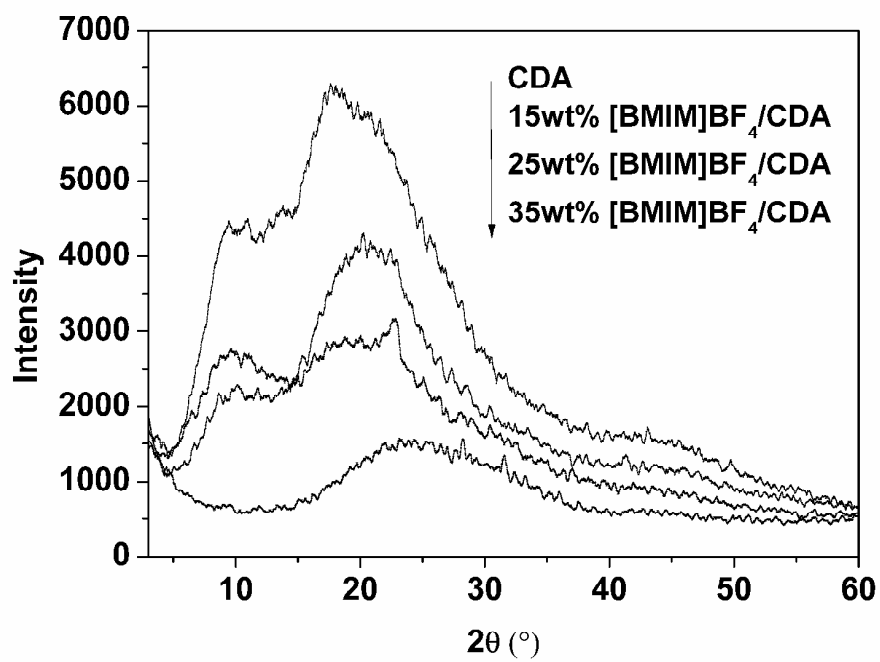


Figure 4

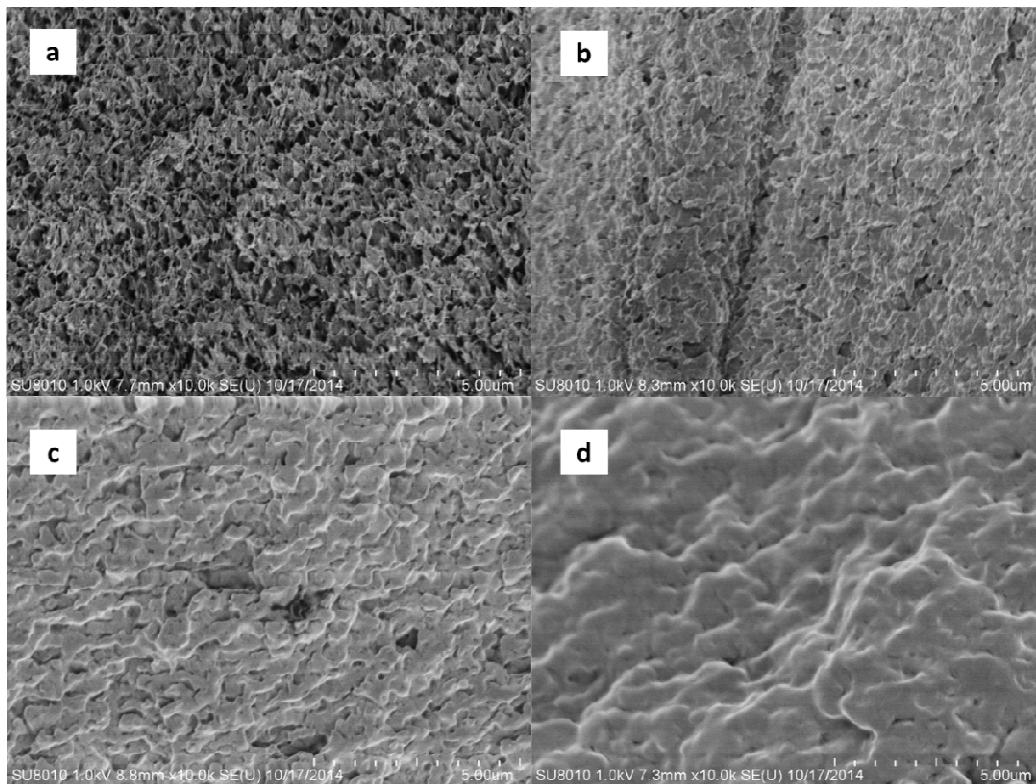


Figure 5

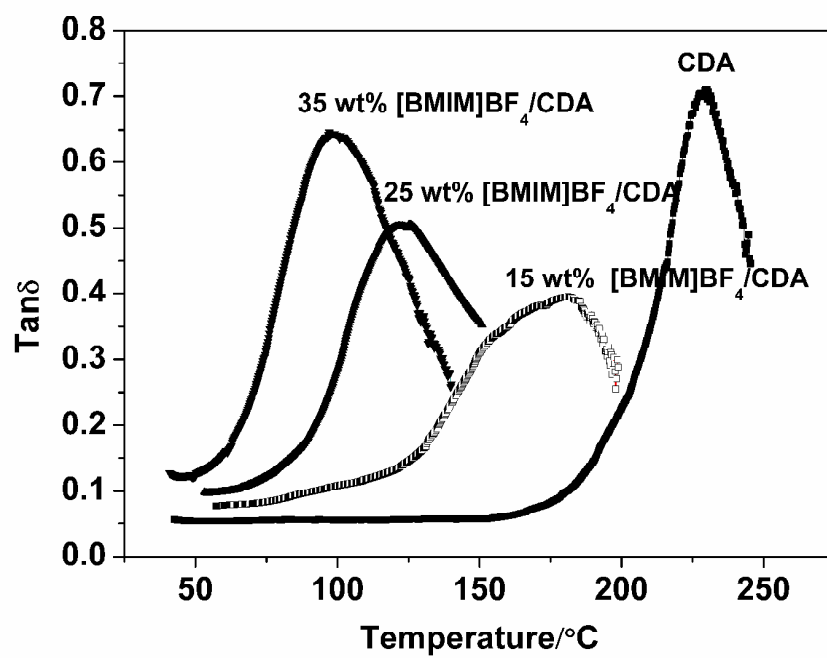


Figure 6

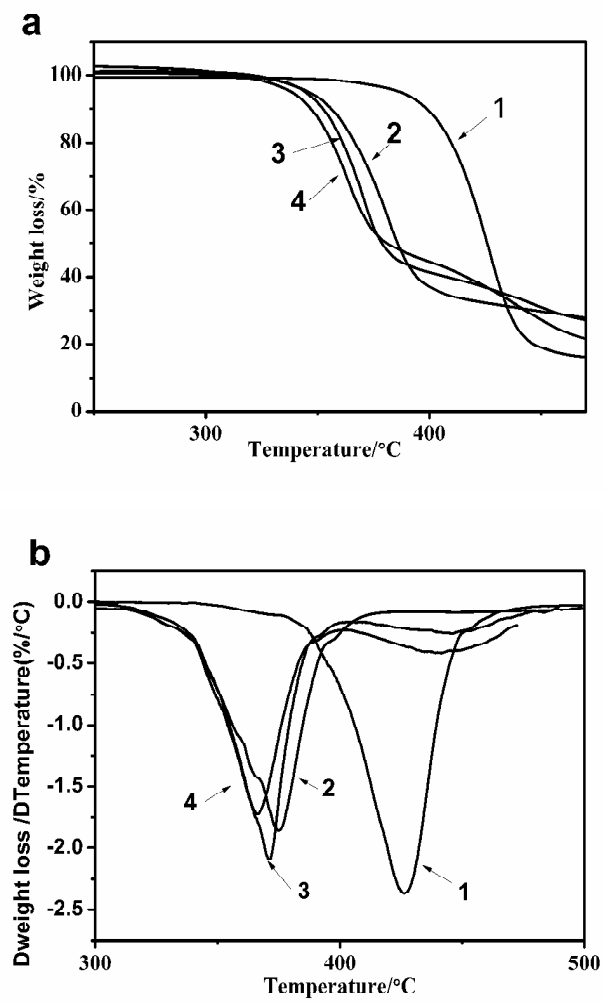


Figure 7

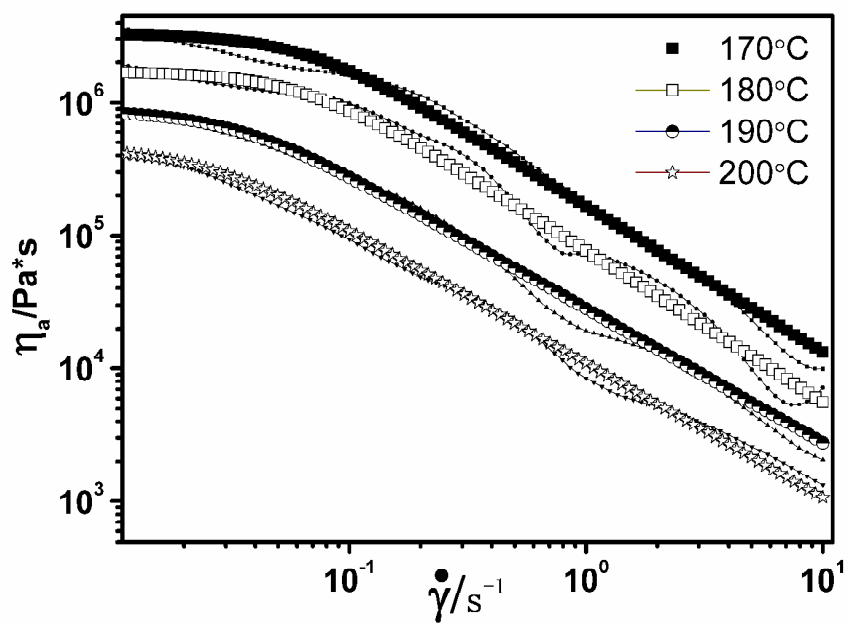


Figure 8

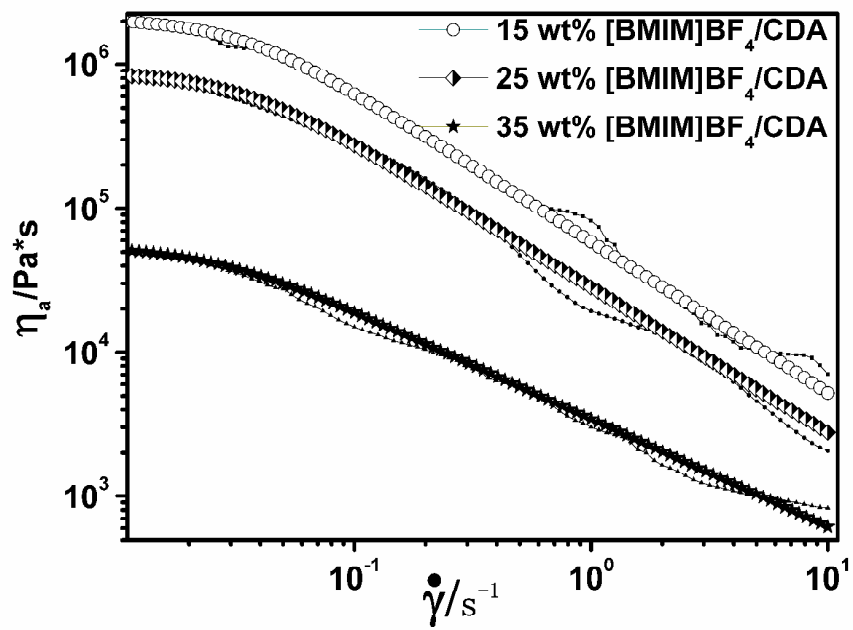


Figure 9

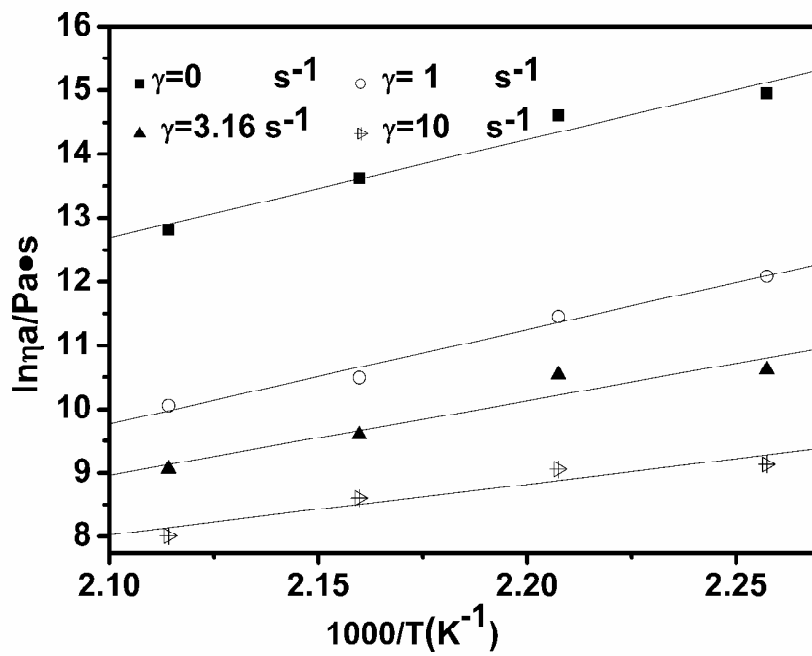


Figure 10

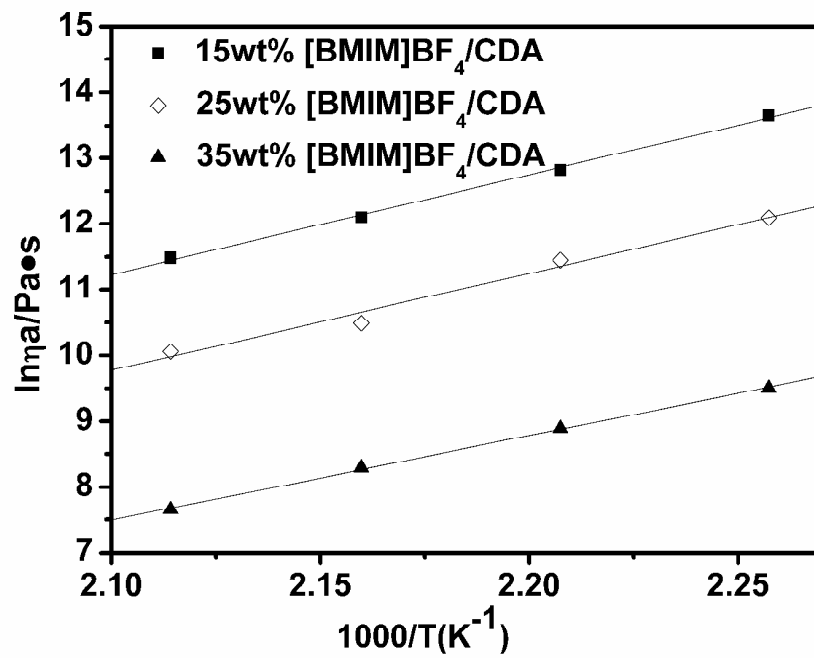


Figure 11

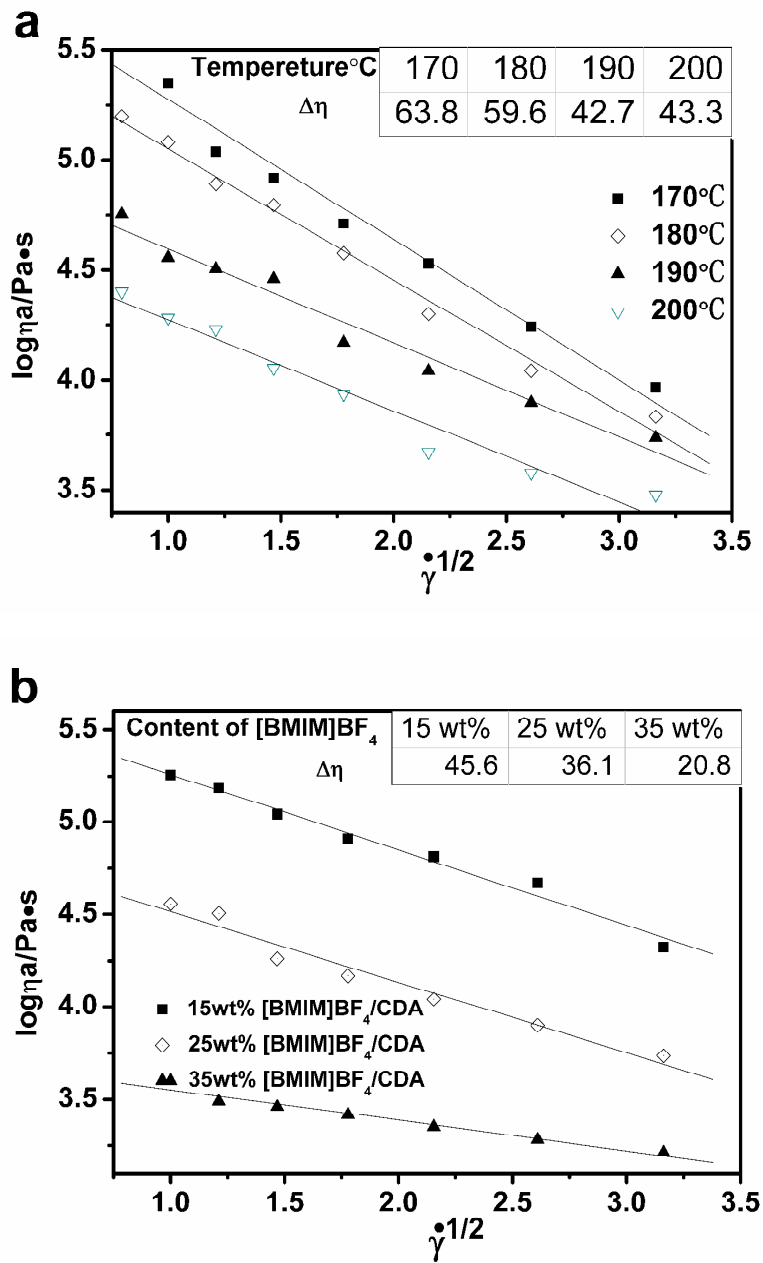


Table 1

Temperature	170°C	180°C	190°C	200°C
$\eta_0/\text{Pa.s}$	3.28×10^6	1.70×10^6	8.78×10^5	4.53×10^5
λ/s	10.11	15.20	23.12	30.42
N	0.48	0.41	0.32	0.30

Table 2

Content of [BMIM]BF ₄	15 wt%	25 wt%	35 wt%
$\eta_0/\text{Pa}\cdot\text{s}$	1.69×10^6	8.78×10^5	5.46×10^4
λ/s	15.71	28.90	40.01
N	0.20	0.32	0.43

Table 3

Shear rate (s^{-1})	0	1	3.16	10
E_{η}/R	15.47	14.78	11.66	7.97
$E_{\eta}/kJ/mol$	128	123	97	66
R_0	0.98127	0.9917	0.9565	0.9492

Table 4

Content of [BMIM]BF ₄	15wt%	25wt%	35wt%
E _η /R	16.14	14.78	12.87
E _η kJ/mol	136	123	107
R ₀	0.9981	0.9917	0.9982